[CANCER RESEARCH 51, 799-806, February 1, 1991]

Multiparametric Flow Cytometry of the Modulation of Tumor Cell Membrane Permeability by Developmental Antitumor Ether Lipid SRI 62-834 in EMT6 Mouse Mammary Tumor and HL-60 Human Promyelocytic Leukemia Cells[1]

Caroline Dive,[2] James V. Watson, and Paul Workman[3]

Medical Research Council Clinical Oncology and Radiotherapeutics Unit, Medical Research Council Centre, Hills Road, Cambridge, CB2 2QH, United Kingdom

ABSTRACT

(+/−)-2-{Hydroxy[tetrahydro-2-(octadecyloxy)methylfuran-2-yl]methoxyl}phosphinyloxy-*N,N,N*-trimethylethaniminium hydroxide, inner salt (SRI 62-834) is a tetrahydrofuran analogue of platelet activating factor (PAF) that is currently entering clinical trial. Like other ether lipids it is of interest as a membrane-active antitumor agent. Here, we have used two-color multiparameter flow cytometry to study simultaneously its effects on cell membrane permeability, intracellular pH, and cell size/structure of EMT6 mouse mammary tumor cells and HL-60 human promyelocytic leukemia cells *in vitro*. Concentrations as low as 1 μM up to 100 μM SRI 62-834 caused a rapid, dose-dependent increase in membrane permeability, initially towards outward efflux of the preloaded fluorescein probe bis(carboxyethyl)carboxyfluorescein (green fluorescence) and then towards influx of extracellular propidium (red fluorescence). At the same time, median cell size from light scatter was reduced with an increased coefficient of variation, and the proportion of cell debris was elevated. *In vitro* antitumor activity was seen over the same concentration range, as measured by tetrazolium dye reduction and cell growth curves. Neither low concentrations of PAF (50 nM) nor the potent PAF antagonist 3-[4-(2-chlorophenyl)-9-methyl-6*H*-thieno[3,2-*f*][1,2,4]triazolo[4,3*a*][1,4]diazepin-2-yl]-1-(4-morpholinyl)-1-propanone (0.5-100 μM) had any influence on the membrane effects of SRI 62-834, and at higher concentrations (1-200 μM) PAF mimicked the behavior of SRI 62-834. In addition, the PAF antagonist did not modulate the cytotoxicity of SRI 62-834 or PAF. HL-60 cells were more sensitive to SRI 62-834 than were EMT6 cells in terms of both cytotoxicity and membrane permeability. However, PAF was more potent than SRI 62-834 in causing membrane permeabilization with both cell lines, whereas PAF was less active than SRI 62-834 in cytotoxicity assays. The results support a membrane-damaging role in the cytotoxicity of SRI 62-834 but suggest that additional factors are also involved. Membrane permeabilization may be related to its reported effects on protein kinase C-dependent intracellular calcium signaling but apparently does not involve a conventional PAF receptor in HL-60 or EMT6 cells.

INTRODUCTION

Ether lipid anticancer agents have now entered Phase 1 clinical trial following encouraging results *in vitro* and in animal studies (1). Examples are ET-18-OCH_3[4] (2) and the cyclic ether analogue SRI 62-834 (3). Both are analogues of the naturally occurring PAF (Fig. 1).

In addition to its potent activation of platelets, PAF exhibits a variety of physiological and pathological effects (4, 5). Ether phospholipid analogues likewise show a diverse range of pharmacological properties, including antiproliferative and cytotoxic effects against human tumor cell lines *in vitro* (6-9), antiinvasive activity *in vitro* (10, 11), antimetastatic activity *in vivo* (12, 13), and immunomodulation in mouse tumor models *in vivo* (1, 14). ET-18-OCH_3 has also been used successfully to purge mouse bone marrow of leukemic cells *in vitro* (15).

The molecular mechanisms by which ether lipid analogues exert these disparate effects are not yet fully understood. Preferential disturbance of phospholipid metabolism in tumor cells has been reported (16, 17). Selectivity may arise from a deficiency in tumor cell membranes of alkyl cleavage enzymes, leading to accumulation of the synthetic lipids (18, 19). This may be responsible for the marked changes in membrane structure and function (11, 20). However, some evidence disputes that cleavage enzyme differences exist in sensitive and resistance cells (21). Effects on signal transduction may also be implicated. ET-18-OCH_3 has been reported to inhibit protein kinase C and to decrease arachidonate release (22), but this was not confirmed for SRI 62-834 (3). The latter has, however, been shown to elicit a time- and concentration-dependent elevation of intracellular calcium in HL-60 human promyelocytic leukemia cells (23, 24).

PAF itself activates pathways involved in coagulation and inflammation at concentrations below nanomolar through to micromolar (4, 5). Other effects are seen at higher concentrations, including for example activation of macrophages at 1-10 μM (25). Differentiation of cultured neurons is seen at 50 nM to 10 μM, but neuronal cell death occurs at higher exposures (26). Potency is generally reduced in the presence of serum proteins.

Although definitive identification of a membrane protein receptor for PAF is lacking, the existence of such receptors is strongly implicated—at least in platelets and neutrophils—by such evidence as high potency, structure-activity relationships, stimulus-specific desensitization, high-affinity saturable binding, and effects of antagonists and antibodies (4). Specific receptor binding is thought to be linked to the PAF-induced increase in cytoplasmic free calcium in platelets, acting by both mobilization of intracellular stores and the opening of a membrane calcium channel (27, 28). However, the structure of PAF and related agents clearly suggests the possibility of detergent-like effects. In fact, recent studies have demonstrated that PAF does act as a general membrane perturbant at concentrations

Received 8/28/89; accepted 11/6/90.

The costs of publication of this article were defrayed in part by the payment of page charges. This article must therefore be hereby marked *advertisement* in accordance with 18 U.S.C. Section 1734 solely to indicate this fact.

[1] This work was supported by the United Kingdom Medical Research Council.

[2] Present address: Pharmaceutical Sciences Institute, Aston University, Birmingham, United Kingdom.

[3] To whom correspondence and requests for reprints should be addressed, at Cancer Research Campaign Department of Medical Oncology, Cancer Research Campaign Beatson Laboratories, University of Glasgow, Garscube Estate, Switchback Road, Glasgow G61 1BD, United Kingdom.

[4] The abbreviations used are: ET-18-OCH_3, 1-*O*-octadecyl-2-*O*-methyl-*rac*-3-phosphocholine; BCECF, bis(carboxyethyl)carboxyfluorescein; BCECF-AM, acetoxy-methyl ester of bis(carboxyethyl)carboxyfluorescein; ID_{50}, ID_{90}, concentrations required for 50% or 90% effect; MTT, 3-(4,5-dimethylthiazol-2-yl)-2,5-diphenyl tetrazolium bromide; PAF, 1-*O*-octadecyl-2-*O*-acetyl-*sn*-glycero-3-phosphocholine; PBS, Dulbecco "A" phosphate-buffered saline; SRI 62-834, (+/−)-2-{hydroxy[tetrahydro-2-(octadecyloxy)methylfuran-2-yl]methoxyl}phosphinyloxy-*N,N,N*-trimethylethaniminium hydroxide, inner salt; also designated CRC 86-05 and NSC 614383; WEB 2086, 3-[4-(2-chlorophenyl)-9-methyl-6H-thieno[3,2-*f*][1,2,4]triazolo[4,3-*a*][1,4]-diazepin-2-yl]-1-(4-morpholinyl)-1-propanone; PI, propidium iodide.

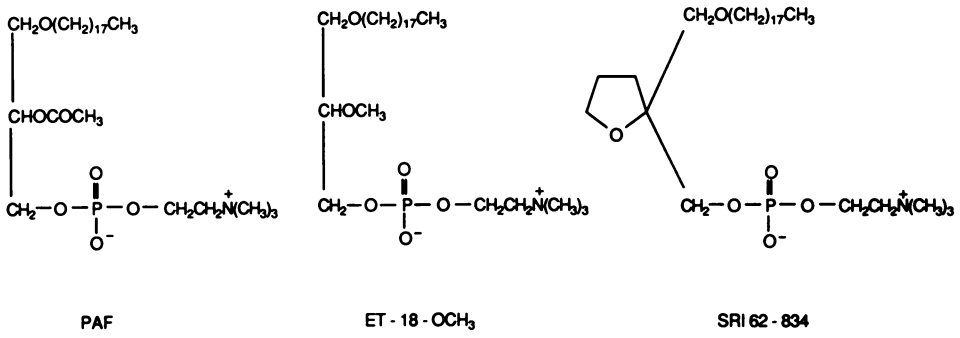

Fig. 1. Molecular structure of ether lipid SRI 62-834 (CRC 86/05; NSC 615 383), ET-18-OCH_3, and platelet activating factor (PAF).

above 4 μM (in protein-free medium), causing a substantial disruption of lipid bilayer structure (29). Clearly such membrane perturbation could also contribute to cell calcium changes, as well as pharmacological and cytotoxic effects.

The *in vitro* antitumor effects of ether lipids such as ET-18-OCH_3 and SRI 62-834 are seen in the concentration range of 1-200 μM in serum-containing medium, and an order of magnitude lower in the absence of serum (1, 30). A PAF antagonist was shown to reduce the cytotoxicity of these ether lipids (30), although this does not necessarily implicate involvement of a PAF receptor. Elevation of intracellular free calcium by ET-18-OCH_3 and SRI 62-834 was seen at 30-140 μM in serum-free medium (23, 24) and although recent results show a lack of modulation of this effect by PAF antagonists (31), the ether lipid-induced calcium rise is reduced by phorbol ester (23, 24). Considering the potential for either receptor-mediated or other specific cell signaling biochemical effects against a more detergent-like biophysical perturbation, further studies are required to elucidate the mechanism of direct antitumor action by ether lipids.

In view of the potential for differential response in discrete tumor cell subpopulations, it is particularly valuable to search for such mechanisms using a cell-by-cell analytical technique such as flow cytometry. Judicious choice of fluorescent probes also permits simultaneous measurement of multiple parameters. We now report the use of our sensitive 2-color multiparameter flow cytometry technique (32) to demonstrate alterations in tumor cell membrane permeability after treatment with SRI 62-834. Progressive modifications of membrane function were identified in tumor cell populations by reduced ability to retain the fluorescein analogue BCECF, followed by increased permeability to extracellular propidium. These sequential changes were shown to be associated with a progressive alteration in cell size or structure as reflected in light scatter properties, but significant pH changes were not seen. To relate the SRI 62-834 concentrations required to modulate cell membrane permeability to those causing *in vitro* antitumor activity, the latter was assessed using the MTT tetrazolium dye reduction assay, cell population growth curve analysis, and clonogenic assay. Membrane permeability effects were seen with SRI 62-834 and also PAF at cytotoxic micromolar concentrations but not in the subtoxic nanomolar range. Neither the membrane permeabilization by SRI 62-834 nor its cytotoxicity was blocked by PAF or the potent and specific PAF antagonist WEB 2086 (33). This was true for EMT6 mouse mammary tumor cells, which were relatively resistant to ether lipids, as well as the more sensitive HL-60 human promyelocytic leukemia line. Both tumor cell lines show a rise in intracellular free calcium in response to SRI 62-834 and PAF (23, 24, 34, 35), and HL-60 cells have been reported to exhibit specific binding of radiolabeled PAF (36).

MATERIALS AND METHODS

Cells

EMT6/VJ mouse mammary tumor cells (37, 38) were cultured in monolayer and prepared as single cell suspensions in Eagle's medium containing 20% newborn calf serum and antibiotics and in an atmosphere of 5% CO_2, 95% air. HL-60 human promyelocytic leukemia cells (23, 24, 36) were grown in suspension culture in antibiotic-free RPMI 1640 containing 10% fetal calf serum and in an atmosphere of 8% CO_2/92% air. Both lines were grown at 37°C and log-phase cells were used throughout.

Drugs

SRI 62-834 and WEB 2086 were gifts from Sandoz Research Institute (East Hanover, NJ) and Boehringer Ingelheim (Ingelheim am Rhein, West Germany), respectively (see "Acknowledgments"). PAF was purchased from Peninsula Laboratories Europe (St. Helens, Merseyside, United Kingdom). These agents were dissolved in PBS at 5 mM and stored at −20°C in the dark. Stock solutions were diluted immediately before use to yield final assay concentrations as appropriate.

Fluorochromes

PI (Sigma, Poole, United Kingdom) and BCECF-AM (Molecular Probes Inc., Eugene, OR) were prepared as stock solutions at 3.0 mM in PBS and 1 mM in dimethyl sulfoxide, respectively, and stored at 4°C in the dark. The BCECF-AM stock solution was diluted with PBS immediately before addition to cells, yielding a final assay concentration of 1 μM. The PI solution was added directly to cell samples so that the final concentration was 30 μM.

Other Reagents

Nigericin was obtained from Sigma, prepared as a stock solution in Grade A ethanol (James Burroughs Ltd., London, United Kingdom) at 1 mM, and stored at 4°C. This solution was added to cell samples to give a final assay concentration of 10 μM. Potassium phosphate buffers of pH 6 to 8 were made by mixing appropriate proportions of 135 mM $KHPO_4$ and 110 mM K_2HPO_4, both containing 20 mM NaCl (all from Sigma) (39). These were stored at 4°C and pH was checked before each experiment. MTT was obtained from Sigma. A stock solution was prepared at 5 mg/ml in PBS and stored at 4°C in the dark.

Flow Cytometry Instrumentation

Full details of the instrumentation and use of the Cambridge Medical Research Council Flow Cytometer are given elsewhere (38, 40, 41). Briefly, the argon laser was set to excite at 488 nm with a power setting of 300 mW. The electronics were instructed to trigger on the 90° light scatter signal. Green fluorescence from liberated BCECF was detected at 515-560 nm and red fluorescence due to DNA-intercalated pro-

pidium at >630 nm. The detector gains were set so that control (nonpermeable) cells were recorded at 2/3 maximum response on the green channel and <100 on the red channel. With these particular settings, the permeable cells were recorded with the G_1 DNA (propidium) peak between channels 450 and 550 and BCECF fluorescence at <100 channels. The small red channel signals in the control (nonpermeable) cells were due to some optical filter breakthrough, and the small signals in the green channel for the permeable cells were due to a combination of residual green fluorescence plus filter breakthrough from the highly intense propidium signals. The green channel detector gain setting was required to be relatively "low" in the experiments in which BCECF plus propidium were being used in combination, in order to minimize red signal breakthrough from the DNA-propidium complex into the green channel. In the experiments in which BCECF was used for pH determinations (when propidium was not present), a 532 ± 2 nm (green) band pass filter was used on this channel and the green detector gain settings were increased considerably to record the low-level residual green fluorescence in the SRI 62-834-treated cells.

At the flow rate used (150-200 cells/s), the probability of coincident cells is extremely low. However, any rare coincident cells and doublets were excluded by electronic double threshold determination together with pulse shape analysis, both on the master detector, while debris was gated on forward and 90° scatter (42). After 10-bit A-D conversion, the data were collected list-mode via PDP LS1-23 and 11-40 computers and stored on hard disc for subsequent analysis. Parameters were selected from green fluorescence, red fluorescence, forward scatter, 90° scatter, and time. Owing to the slit-scan effect, the integrated areas under the fluorescence pulses were analyzed. In-house programs were used to display processed data as 2-parameter frequency contour plots or as perspective 3-dimensional plots of 2 selected parameters together with cell frequency. In cases where cell subpopulations were identified from analysis of 2 parameters (*e.g.*, red *versus* green fluorescence), other selected parameters (*e.g.*, forward-angle light scatter) were investigated as appropriate by electronic gated analysis. Data presented in the figures have linear coordinates. All flow cytometry procedures were carried out at room temperature unless stated otherwise.

Effects of SRI 62-834 on Permeability to BCECF and PI

Cells were loaded with 1 μM BCECF-AM for 5 min and washed to remove excess substrate (43). SRI 62-834 (1-200 μM) and PI (30 μM) were then added and 10,000 cells were analyzed per sample, both immediately and after 15 min with respect to green and red fluorescence, together with forward and 90° light scatter (32).

Effects of SRI 62-834 on Intracellular pH

The method for intracellular pH measurement relies on the pH dependence of BCECF fluorescence emission at around 530 nm (green) but not above 630 nm (red) (39). EMT6 cells were loaded with BCECF as above. Calibration samples were resuspended in potassium phosphate buffers of known pH in the presence of the potassium ionophore nigericin (10 μM) to equalize intra- and extracellular pH. BCECF fluorescence was recorded for 10,000 cells/sample, both at 532 ± 2 nm using a laserline filter (Glen Creston, Dalston, United Kingdom) and simultaneously above 630 nm. Triplicate samples were analyzed. A calibration curve was constructed of pH *versus* the ratio of the median fluorescence above 630 nm to that at 532 ± 2 nm. Using the same instrument settings for these particular experiments, BCECF-loaded cells suspended in medium or in PBS were analyzed in the absence of nigericin with and without SRI 62-834. In some experiments nigericin was added after the effects of SRI 62-834 had been analyzed, in order to determine whether the ionophore could re-establish BCECF fluorescence in the green-negative, red-negative population.

Cytotoxic Effects of SRI 62-834 against EMT6 Cells

The direct effects of SRI 62-834 on log phase EMT6 cells were investigated using 3 different *in vitro* assay procedures.

MTT Assay. This is based on the conversion of the yellow water-soluble tetrazolium salt MTT to a purple insoluble formazan product, catalyzed by dehydrogenases present in viable cells (44, 45). Absorbance is proportional to cell number. Cells (600/well for EMT6 and 2×10^3/well for HL-60) were incubated for 3 (EMT6) or 4 days (HL-60) in the presence of 1-100 μM SRI 62-834. After removal of the medium, a volume of 200 μl MTT solution (5 mg/ml) was added for 6 h. The purple formazan crystals were dissolved in 200 μl of dimethyl sulfoxide and the plates were read in an enzyme-linked immunosorbent assay plate reader at a test wavelength of 540 nm and a reference of 690 nm. Eight replicate wells were used at each individual drug concentration. Results were expressed as the percentage of absorbance compared with the untreated control. This was plotted against the log of the drug concentration to generate dose-response curves from which values of ID_{50} and ID_{90} were determined as the concentrations to reduce the control absorbance by 50 and 90%, respectively.

Clonogenic Cell Survival Assay. Log-phase EMT6 cells were seeded on day 0 at 5×10^4 cells/25-cm² flask with 5 ml of medium. On day 3, the monolayers were treated with 0.1 to 200 μM SRI 62-834. After either 15 or 60 min, the medium was removed and cells were trypsinized, counted with a hemacytometer counting chamber, and appropriate dilutions made. Aliquots of the cell dilutions (1 ml) were added to 9 ml of medium in 9-cm-diameter plastic dishes. Two or 3 replicates were included for each drug concentration. The dishes were incubated for 9 days. After this, the medium was removed and the resulting colonies visualized by crystal violet staining. Colonies of greater than 50 cells were counted using a microscope, and results were expressed as the number of colonies as a proportion of cells plated.

Population Growth Curve Assay. EMT6 cells were seeded in 25-cm² flasks as above, and left for 1 h to allow a monolayer to attach to the plastic surface. SRI 62-834 was then added at 5-100 μM, with 10 replicate flasks per concentration. On day 3, the medium containing any remaining SRI 62-834 was removed, and 5 ml of fresh drug-free medium were added. The cells were subsequently fed with fresh medium each day. On each of the following 8 days, cells from one flask per group were trypsinized, resuspended in medium, and the cell number per flask calculated from hemacytometer counts. This was plotted against time to generate growth curves. Trypan blue dye exclusion tests were performed daily on the trypsinized cells and those present in the aspirated growth medium.

RESULTS

Effects of SRI 62-834 on Tumor Cell Membrane Permeability

Fig. 2 shows 2-parameter frequency contour plots of green BCECF fluorescence (515-560 nm) against red fluorescence due to DNA-intercalated propidium (>630 nm) for EMT6 mouse mammary tumor cells. Three cell populations were seen for all samples, including control cells (32). Region 1 cells exhibit green but no red fluorescence, indicating retention of BCECF and exclusion of propidium. Region 2 cells have little red or green fluorescence, which we interpret as a loss of BCECF but persistence of propidium exclusion (32). Region 3 cells exhibit red but not green fluorescence, suggesting BCECF loss together with a newly developed permeability to propidium.

The effects of increasing SRI 62-834 concentrations (1-50 μM) on this twin-probe fluorescence pattern are illustrated in Fig. 2. Samples were analyzed either immediately or 15 min after drug treatment. No significant change in fluorescence was seen over 15 min for untreated control cells. Increasing SRI 62-834 concentrations caused an immediate and concentration-dependent loss of green fluorescence. The decrease in the number of cells in Region 1 (green positive, red negative) was accompanied by an increase in the cell numbers for Regions 2 (green negative, red negative) and 3 (green negative, red positive). Few cells remained in Region 1 immediately after SRI 62-834 addition at 25 and 50 μM. In no case were cells seen in the center of the isometric plot, *i.e.*, displaying both red and

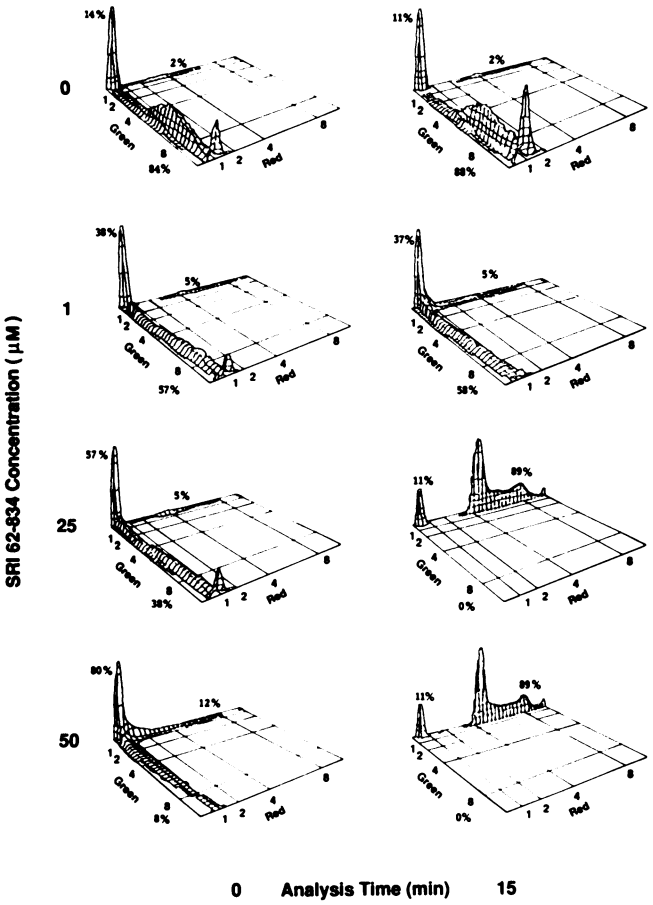

Fig. 2. Effect of SRI 62-834 on the retention of BCECF and the exclusion of propidium by EMT6 mouse mammary tumor cells measured by flow cytometry. Green fluorescence between 515 and 560 nm liberated from BCECF (arbitrary units, channel number) is plotted *versus* red fluorescence above 630 nm due to DNA-intercalated propidium (arbitrary units, channel number) with cell frequency on the vertical axis. Cells (10,000) were loaded with BCECF, exposed to PI, and analyzed immediately or 15 min after addition of the appropriate volume of PBS alone for control cells or of SRI 62-834-treated cells at various concentrations, as shown. The percentages of cells in 3 defined regions (see text) are indicated. Data are from 1 of 3 independent repeat experiments, each of which gave similar results.

green fluorescence simultaneously.

After 15 min in the presence of 1 μM SRI 62-834, the fluorescence distribution of the cells was unchanged with respect to the immediate analysis. Above this drug concentration greater effects were seen after 15-min incubation. For both 25 and 50 μM treatments, no cells remained in Region 1 after 15 min, *i.e.*, all green fluorescence was lost. Clearly recognizable DNA histograms with G_1, S, and G_2 + M peaks were seen on the red fluorescence axis for the latter 2 samples. The proportions of cells in each of the 3 regions are shown in Fig. 2. No further changes occurred with longer exposures. Additional experiments were carried out to determine the effects of SRI 62-834 at concentrations below 1 μM. No modulation of membrane permeability was seen at 35 or 50 nM.

A secondary electronic gating procedure was carried out to assess the forward and 90° scatter profiles, related to cell size and shape, for the 3 discrete subpopulations exhibiting different fluorochrome staining. Green negative, red positive cells (Region 1, "intact membranes") displayed discrete frequency-scatter profiles. Green negative, red positive cells (Region 3) exhibited a wide variation in light scatter, consistent with having severely damaged membranes. Green negative, red negative cells (Region 2) showed an intermediate frequency-scatter profile.

Membrane permeability changes closely similar to those described for EMT6 cells were also seen for SRI 62-834-treated HL-60 human promyelocytic leukemia cells. However, HL-60 was at least 2.5-fold more sensitive. A concentration of 10 μM caused a complete loss of green fluorescence after 15 min compared with only 50% loss for EMT6.

All of the experiments described above were carried out at room temperature. In addition, experiments were performed in which cell samples were either maintained at room temperature before and during flow cytometry or held at room temperature until immediately before fluorescence analysis. The results (not shown) were closely similar for the tested concentrations of 25-150 μM SRI 62-834.

Influence of PAF and its Antagonist WEB 2086 on Membrane Permeabilization by SRI 62-834

A series of experiments was performed to determine the effects of PAF and WEB 2086, alone or in combination with SRI 62-834. When tested alone, PAF had no effect on membrane permeability at very low concentrations (35 and 50 nM). At micromolar concentrations, PAF gave a similar pattern of response to SRI 62-834 in both EMT6 and HL-60, but was about twice as potent. The PAF antagonist WEB 2086 had no effect by itself at concentrations of 0.5-100 μM. Such levels are well above those reported (33) to block PAF-induced human platelet and neutrophil aggregation *in vitro* (ID_{50} values, 0.17 and 0.36 μM, respectively). However, these concentrations failed to modulate membrane permeabilization of EMT6 and HL-60 cells by 50-200 μM SRI 62-834 or 25-100 μM PAF (not shown). In addition, low concentrations (50 nM) of PAF failed to block the membrane effects of SRI 62-834 and higher concentrations (100-200 μM), which were themselves membrane-active, gave an additive response with SRI 62-834 (not shown).

Effects of SRI 62-834 on Intracellular pH

Since BCECF fluorescence is pH-sensitive, it was possible that the decrease in green fluorescence brought about by SRI 62-834 was due to a change in intracellular pH. We therefore compared the effects of the drug on BCECF fluorescence at 532 ± 2 nm (pH-sensitive green region) to that above 630 nm (pH-insensitive red region). This was done in the absence of PI. Cells exhibiting light scatter characteristics consistent with dead or dying cells were gated out and ignored in the analysis of fluorescence.

The red/green fluorescence ratio obtained for untreated control EMT6 cells was highly reproducible with a mean value of 1.40 and an SD of 0.017 (coefficient of variation = 1.2%) for a total of 17 different samples analyzed in 3 separate experiments. By reference to calibration standards using the ionophore nigericin, this was shown to correspond to an intracellular pH of 7.40. In general, SRI 62-834 produced a similar reduction in BCECF fluorescence at both wavelengths. Typical pH values for control and drug-treated cells were 7.40 and 7.35, respectively. In no case was the fluorescence ratio decreased by more than 0.03 compared with the average control ratio for any samples analyzed immediately after 1-60 μM SRI 62-834. This corresponded to a maximum reduction in pH of only 0.05 pH units, *i.e.*, to pH 7.35.

Experiments were also carried out in which cells were first treated with SRI 62-834 so as to induce a loss of BCECF, and

the effect of adding nigericin was then determined. The ether lipid-induced lack of BCECF fluorescence in the green-negative population was unaffected by nigericin, ruling out a pH effect and confirming that the predominant cause is the modulation of membrane permeability by SRI 62-834.

Cytotoxicity of SRI 62-834 on EMT6 and HL-60 Cells

MTT Assay. Fig. 3*A* shows the cytotoxic effect of SRI 62-834 on EMT6 cells using the MTT assay. The ID_{50} and ID_{90} values were 26 and 80 μM, respectively, and at 100 μM SRI 62-834 the absorbance was reduced by 96% (mean, 5 experiments). SRI 62-834 showed more potent activity in HL-60 cells, with a mean ID_{50} value of 2.5 μM (n = 4). In both cell lines, PAF was less active than in SRI 62-834, the ID_{50} values being 230 μM for EMT6 (n = 2) and 59 μM for HL-60 (n = 4).

The effects of PAF antagonist WEB 2086 on the cytotoxic response of EMT6 and HL-60 cells were also determined. WEB 2086 was only weakly cytotoxic with an ID_{50} value in the region of 300 μM for HL-60 cells and >100 μM for EMT6 cells. Tested at 1, 10, and 100 μM concentrations, WEB 2086 was reproducibly without effect on the cytotoxicity of either SRI 62-834 or PAF in either cell lines (n = 3, not shown).

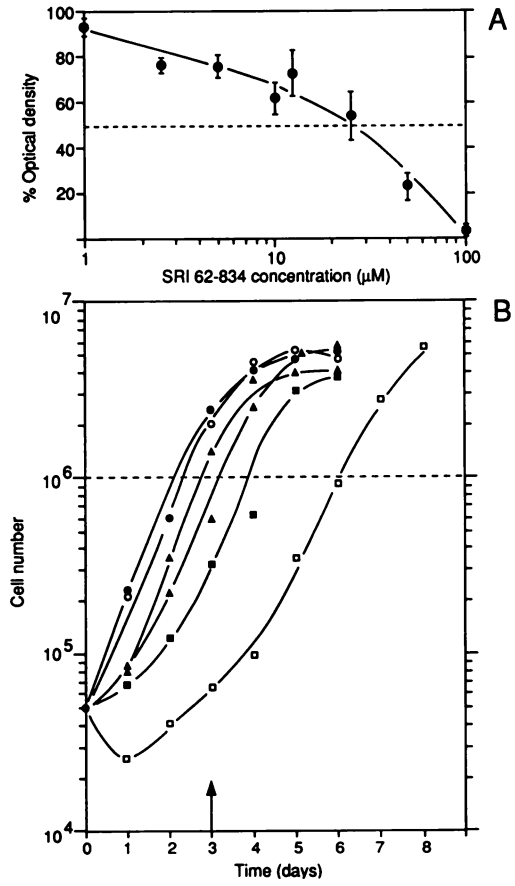

Fig. 3. *In vitro* cytotoxicity of SRI 62-834 in EMT6 tumor cells. *A*, measured by the MTT assay. Results are expressed as dose-response curves of percentage of absorbance with respect to untreated controls against the drug concentration added to the medium. *Points*, mean of pooled results from 5 independent experiments; *bars*, 2 SE. In each experiment, average values were calculated from 8 replicate samples. ID_{50} values are marked by the *broken lines B*, determined by population growth curve analysis. Cultures were set up from initial inocula of 5 × 10^4 on day 0. Cells were untreated (*closed circles*) or treated for 3 days with SRI 62-834 at concentrations of 5 μM (*open circles*), 15 μM (*closed triangles*), 30 μM (*open triangles*), 60 μM (*closed squares*), and 100 μM (*open squares*). The *dotted line* allows comparison of the time taken for each treatment group to reach 10^6 cells, and the *arrow* at day 3 indicates the time of removal of any remaining ether lipid. Results are from 1 of 2 independent experiments.

Clonogenic Cell Survival Assay. In all cases, the number of colonies formed as a proportion of intact EMT6 cells plated was closely similar to control values for 15- and 60-min exposures in the concentration range 0.1-200 μM SRI 62-834. For example, analysis of pooled data from 3 independent experiments, with 2-3 replicate plates in each, gave plating efficiencies of 95 ± 1.8% (SE, n = 18) for controls and 94 ± 1.8% (SE, n = 12) for 200 μM SRI 62-834.

Cell Population Growth Curve Assay. Fig. 3*B* shows the growth curves, from 1 of 2 repeat experiments, for control cells and those treated with SRI 62-834 at 5-100 μM. Exponential growth was seen for control cells up to 3.5 days, following which a plateau phase was observed. Cells treated with 5 μM SRI 62-834 exhibited a growth pattern closely similar to that of control cells. A concentration-dependent retardation of growth was seen for ether lipid treatment at 15-60 μM. At these doses, exponential growth parallel to the control curve was preceded by a lag phase. Treatment with 100 μM SRI 62-834 caused a 3-fold decrease in cell number from the initial 5 × 10^4 inoculum to about 1.7 × 10^4 cells counted on day 1. The time of cell doubling from 5 × 10^5 to 10^6 was about 12 h for all groups, but the time required to amass 10^6 cells increased progressively with drug concentration (Table 1). Using this as an end point, growth delays of approximately 2 and 4 days, respectively, were obtained for 60 and 100 μM SRI 62-834 (Table 1). Approximate ID_{50} and ID_{90} values of 25 and 66 μM were obtained from the plot of percentage of cells per flask on day 3 *versus* SRI 62-834 concentration. These values were closely similar to those obtained by MTT assay.

Trypan blue dye exclusion tests showed that the percentage of "nonviable" cells (*i.e.*, those including the dye) increased from 0-2% on days 1-4 to up to 8% by day 6 for SRI 62-834-treated and control cells alike. No cells were seen in the growth medium aspirated before trypsinization of the monolayers. For SRI 62-834 concentrations of 60 and 100 μM, visual inspection on days 1-3 revealed that 10 and 60% of cells, respectively, had swollen to approximately 4 times their original diameter. After the medium change on day 3, the number of these abnormally large cells gradually decreased, but approximately 10% still remained on day 8 after exposure to 100 μM SRI 62-834.

The decrease in cell number seen on day 1 after 100 μM lipid treatment suggests an immediate cytolytic action of the drug at this higher concentration. This is endorsed by the large increase in the number of cells exhibiting minimal light scattering ability measured by flow cytometry, from about 3% for control cells to about 85% in the presence of ether lipid 15 min after drug addition at 100 μM.

DISCUSSION

The principal object of this work was to investigate the effects of the developmental ether lipid analogue SRI 62-834 on the permeability dynamics of the cell membrane of EMT6 mouse

Table 1 *Effect of ether lipid SRI 62-834 on EMT6 cell growth*[a]

Initial concentration of SRI 62-834 (μM)	Time for cell no. to increase from 5 × 10^4 to 10^6 cells (h)	Growth delay (h)
0	55.2, 57.6	0, 0
5	58.2, 58.8	3.0, 1.2
15	64.8, 61.2	9.6, 3.6
30	80.4, 75.6	25.2, 18.0
60	100.8, 98.4	45.6, 40.8
100	146.4, 158.4	91.2, 100.8

[a] Values shown are from 2 independent experiments.

mammary tumor cells and HL-60 promyelocytic leukemia cells using 2-color multiparameter flow cytometry. To shed light on possible mechanisms, the effects of PAF itself and of the PAF antagonist WEB 2086 on membrane permeabilization by SRI 62-834 were also determined. Modification of intracellular pH and cell size/shape were also examined. An additional aim was to correlate the concentrations required to bring about these changes with those required for the antiproliferative effects of the drug, also reported here for the same 2 cell lines.

Using BCECF combined with PI as complementary fluorescent probes for the sensitive multiparametric analysis of cell membrane permeability, it was previously shown that 3 distinct membrane permeability states can be defined operationally within a heterogenous population of EMT6 cells (32). Since a variety of evidence suggests that SRI 62-834 acts primarily on cancer cell membranes (1, 11, 20), we expected to see a change in permeability towards the relatively large, charged probe fluorochromes, leading to an altered distribution across the 3 discrete membrane permeability states. Addition of SRI 62-834 did indeed cause a rapid change in the fluorescence properties of EMT6 cells preloaded with BCECF and then exposed to PI. In particular, a loss of green signal preceded a gain in red fluorescence. The alterations were both drug concentration- and exposure time-dependent. No cells were seen with the ability simultaneously to fluoresce red and green in the presence of up to 50 μM SRI 62-834. This demonstrated the absolute requirement to traverse an intermediate membrane permeability state where cells have lost the ability to retain BCECF but nevertheless remain impermeable to propidium, and hence exhibit minimal green or red fluorescence.

The above data strongly suggested a drug-induced increase in membrane permeability to BCECF. However, since BCECF fluorescence is pH-sensitive in the green, the possibility existed that the decrease in fluorescence seen at 515-560 nm might be caused by a reduction in intracellular pH. However, even after exposure to 100 μM SRI 62-834 for 15 min, the maximal decrease in pH in the population undergoing a progressive loss of BCECF was from 7.40 to 7.35. A considerably larger pH reduction of pH 7.5 to 7.2 results in only a 15% decrease in fluorescence (46). Furthermore, the proton ionophore nigericin was unable to restore green fluorescence to the negative population in Region 2. Thus, increased membrane permeability is the major mechanism for the loss in green BCECF fluorescence at 515-560 nm.

Five-parameter gated analysis incorporating forward and 90° light scatter measurement provided information on drug-induced changes in cell size and shape among the subpopulations differing in membrane permeability. Cells scoring as green positive, red negative ("intact membranes") were uniform in size as indicated by discrete frequency *versus* scatter distribution. Those registering green negative, red positive exhibited a wide variation in light scatter, consistent with their interpretation as severely damaged cells (32). The light scatter profile for the green negative, red negative population showed an intermediate spread of size, in agreement with their classification as cells exhibiting partially perturbed membrane permeability properties.

Membrane permeabilization by SRI 62-834 was observed in the concentration range 1-100 μM for EMT6 and HL-60 cells, the latter being rather more sensitive. PAF itself also caused membrane permeabilization with twice the potency of SRI 62-834. For neither agent were effects seen at 35-50 nM. Such low concentrations of PAF also failed to affect membrane permeabilization by SRI 62-834. Importantly, the potent thieno-triazolodiazepine PAF antagonist WEB 2086 was likewise without influence on the membrane permeability effects of either PAF or SRI 62-834 at antagonist concentrations well above those that block human platelet and neutrophil aggregation *in vitro* (33).

It is important to emphasize that the micromolar concentration ranges used in the present experiments (all performed with serum-containing media) were similar for both membrane permeability and cytotoxicity. Using the MTT assay the ID_{50} and ID_{90} values in EMT6 cells were 26 μM and 80 μM SRI 62-834, respectively after a nominal drug exposure time of 3 days. Maximal effect was seen at 100 μM ether lipid. In cell proliferation assays, growth curves were parallel to controls in all cases, and delays of 2-4 days were determined for 60-100 μM SRI 62-834. ID_{50} and ID_{90} values were closely similar to those for the MTT assay at 25 and 66 μM, respectively. Clonogenic assays carried out after 15- or 60-min exposures showed that, as a proportion of cells plated, there was no difference in the number of colonies produced from the control and SRI 62-834-treated cells (about 94%).

Taken together with the flow cytometric demonstration of dose-dependent increase in propidium staining, altered light scatter profile and increased proportion of cell debris, the results are indicative of a rapid, membrane-targeted cytolytic effect. Severely membrane-damaged cells would be removed before and during trypsinization and not detected by clonogenic assay. The effects seen in the MTT and population growth curve assays can therefore be attributed to this rapid cytolytic effect. For cells that survive such damage, clonogenic survival is identical to controls. However, although in the population growth studies most cells were viable by trypan blue exclusion, an increasing proportion did fail to exclude dye with escalating ether lipid doses, and there was also a dose-dependent increase in the number of cells exhibiting a swollen appearance at day 3. This suggests some residual biological effect of the drug on a proportion of surviving cells.

HL-60 cells were much more sensitive to SRI 62-834 cytotoxicity (ID_{50} of 2.5 μM compared with 26 μM for EMT6), in line with their different susceptibilities to membrane permeabilization. On the other hand, PAF was markedly less potent than SRI 62-834 in each cell line (ID_{50} values, 59 μM for HL-60 and 230 μM for EMT6), although it was more potent in terms of membrane permeabilization. However, in keeping with the membrane permeability results, WEB 2086 was shown not to affect response to PAF or SRI 62-834 in either HL-60 or EMT6 cells. The results support a membrane-damaging role in the cytotoxicity of SRI 62-834 but suggest that additional mechanisms may be at work. These events do not, however, involve a conventional PAF receptor.

The precise mechanisms involved in these initially subtle and progressively more severe membrane damage events are not clear. Sustained elevation of intracellular calcium by 30 μM SRI 62-834 has been reported for human promyelocytic HL-60 cells in serum-free medium, together with antagonism by the protein kinase C-activating phorbol ester 12-*O*-tetra-decanoyl-phorbol-13-acetate but not the PAF antagonist L-652,731 (23, 24, 31). We have also seen elevated intracellular calcium in EMT6 cells at SRI 62-834 doses that cause only modest changes in cell permeability in serum-containing medium (34, 35). The greater susceptibility of HL-60 cells to membrane permeabilization by SRI 62-834 is consistent not only with the cytotoxicity data, but also with their higher sensitivity to intracellular calcium

elevation.[5] It seems possible that SRI 62-834 and related agents undergo an initially subtle interaction with the cell membrane, leading to an elevation in intracellular free calcium prior to more extensive modification of membrane structure and function. However, for Swiss 3T3 fibroblasts in the presence of serum, only a transient increase in calcium was seen with ET-18-OCH_3 (47).

Accumulating data from a variety of cell lines and various assays (see above) suggests that a PAF receptor is probably not involved in the effects of ether lipids on cancer cells. The relative potencies for cytotoxicity and the lack of correlation with PAF agonist behavior also support this view. Although one of the lines used here, HL-60, is known to show PAF binding (36), it would nevertheless be valuable to identify a tumor cell line more similar in PAF receptor status to the platelet. The calcium rise induced by ether lipids appears to involve both an initial release from intracellular stores and the subsequent opening of a verapamil/prenylamine-insensitive membrane calcium channel in HL-60 cells (24). The appearance of a calcium rise, which precedes increased permeability to BCECF and propidium (34, 35), together with a blockade of the calcium rise by protein kinase C-activating phorbol ester, suggest that specific biochemical signaling processes may yet be involved, despite the nonparticipation of a PAF receptor. On the other hand, whereas such biochemical effects may predominate at low drug concentrations, higher exposures may bring about a more severe detergent-like interaction. Clearly, differences in the sensitivities of various cell types to agents like SRI 62-834 may relate to such factors as the extent of the calcium rise and the sensitivity to such elevation, as well as the structure of the cell membrane. Studies are underway to elucidate the sequences of events between calcium elevation, altered membrane permeability, and cell death. Multiparametric flow cytometry is particularly suited to this, since the alteration in a variety of parameters can be studied simultaneously (membrane permeability, cell size/shape, intracellular pH, and Ca^{2+}). In addition, these changes can be measured in multiple discrete cell subpopulations that may exhibit differential responses (*e.g.*, calcium release *versus* membrane lysis).

Regardless of the mechanism, differential sensitivity between various cell lines suggests the possibility of a selective therapeutic effect against particular tumor cell types.

ACKNOWLEDGMENTS

SRI 62-834 is undergoing development under the auspices of the United Kingdom Cancer Research Campaign Phase I/II Clinical Trials Committee and was kindly supplied, via Professor Brian Fox and Professor John Hickman, by Dr. Bill Houlihan of Sandoz Research Institute, East Hanover, NJ. WEB 2086 was a gift from Dr. Karl-Heinz Weber, Boehringer Ingelheim, Ingelheim am Rhein, West Germany. We also thank John Hickman and colleagues for helpful discussions and the sharing of results in advance of publication. Jane Donaldson and Hilary Cox provided expert technical assistance.

REFERENCES

1. Berdel, W. E., Bausert, W. R. E., Fink, U., Rastetter, J., and Munder, P. G. Antitumor action of alkyl-lysophospholipids (review). Anticancer Res., *1:* 345–352, 1981.
2. Berdel, W. E., Fink, U., and Rastetter, J. Clinical Phase I pilot study of the alkyl lysophospholipid derivative Et-18-OCH_3. Lipids, *22:* 966-968, 1987.
3. Houlihan, W. J., Lee, M. L., Munder, P. G., Nemecek, G. M., Handley, D. A., Winslow, C. M., Happy, J., and Jaeggi, C. Antitumor activity of SRI 62–834, a cyclic ether analog of Et-18-OCH_3. Lipids, *22:* 884–890, 1987.
4. Winslow, C. M., and Lee, M. L. (eds.). New Horizons in Platelet Activating Factor Research. Chichester: Wiley, 1987.
5. Beneveniste, J., and Vargaftig, B. B. Platelet activating factor: an ether lipid with biological activity. *In:* H. K. Mangold and F. Paltauf (eds.), Ether Lipids: Biochemical and Biomedical Aspects, pp. 335–376. Academic Press Inc., 1983.
6. Noseda, A., Berens, M. E., Piantadosi, C., and Modest, E. J. Neoplastic cell inhibition with new ether lipid analogs. Lipids, *22:* 878–883, 1987.
7. Andreesen, R., Molodell, M., Weltzien, H. U., Eibl, H., Comman, H. H., Lohr, G. W., and Munder, P. G. Selective destruction of human leukemic cells by alkyl-lysophospholipids. Cancer Res., *38:* 3894–3899, 1978.
8. Berdel, W. E., Fromm, M., Fink, U., Pahlke, W., Bicker, U., Reichert, A., and Rastetter, J. Cytotoxicity of thioether-lysophospholipids in leukemias and tumors of human origin. Cancer Res., *43:* 5538–5543, 1983.
9. Hoffman, D. R., Hadju, J., and Snyder, F. Cytotoxicity of platelet activating factor and related alkyl-phospholipid analogs in human leukemia cells, polymorphonuclear neutrophils, and skin fibroblasts. Blood, *63:* 545–552, 1984.
10. Storme, G. A., Berdel, W. E., van Blitterswijk, W. J., Bruyneel, E. A., de Bruyme, G. K., and Mareel, M. M. Antiinvasive effect of racemic 1-*O*-octadecyl-2-*O*-methylglycero-3-phosphocholine on MO4 mouse fibrosarcoma *in vitro*. Cancer Res., *45:* 351–357, 1985.
11. van Blitterswijk, W. J., Hilkmann, H., and Storme, G. A. Accumulation of an alkyl lysophospholipid in tumor cell membranes affects membrane fluidity and tumor cell invasion. Lipids, *22:* 820–823, 1987.
12. Talmadge, J. E., Schneider, M., Lenz, B., Phillips, H., and Long, C. Immunomodulatory and therapeutic properties of alkyl lysophospholipids in mice. Lipids, *22:* 871–877, 1987.
13. Berdel, W. E., Bausert, W. R. E., Weltzien, H. U., Molodell, M. L., Widman, K. H., and Munder, P. G. The influence of alkyl-lysophospholipids and lysophospholipid-activated macrophages on the development of metastasis of 3-Lewis lung carcinoma. Eur. J. Cancer, *16:* 1199–1204, 1980.
14. Yamamoto, N., and Ngwenya, B. Z. Activation of mouse peritoneal macrophages by lysophospholipids and ether derivatives of neutral lipids and phospholipids. Cancer Res., *47:* 2008–2013, 1987.
15. Glasser, L., Somberg, L. B., and Vogler, W. R. Purging murine leukemic marrow with alkyl-lysophospholipids. Blood, *64:* 1288–1291, 1984.
16. Molodell, M., Andreesen, R., Palke, W., Brigger, U., and Munder, P. G. Disturbance of phospholipid metabolism during the selective destruction of tumor cells induced by alkyl-phospholipids. Cancer Res., *39:* 4681–4686, 1979.
17. Herrmann, B. D. J., and Neumann, H. A. Cytotoxic ether phospholipids. Different affinities to lysophosphocholine acyltransferases in sensitive and resistant cells. J. Biol. Chem., *261:* 7742–7747, 1986.
18. Soodsma, J. F., Piantadosi, G. B., and Snyder, F. The biocleavage of alkylglyceryl ethers in Morris hepatomas and other transplantable neoplasms. Cancer Res., *30:* 309–311, 1970.
19. Berdel, W. E., Greiner, E., Fink, U., Stavrou, D., Reichert, A., Rastetter, J., Hoffman, D., and Snyder. F. Cytotoxicity of alkyl-lysophospholipid derivatives and low-alkyl-cleavage enzyme activities in rat brain tumor cells. Cancer Res., *43:* 541–545, 1983.
20. Noseda, A., Godwin, P. L., and Modest, E. J. Effects of antineoplastic ether lipids on model and biological membranes. Biochim. Biophys. Acta, *945:* 92–100, 1988.
21. Wilcox, R. W., Wykle, R. L., Schmitt, J. D., and Daniel, L. W. The degradation of platelet activating factor and related lipids: susceptibility to phospholipases C and D. Lipids, *22:* 800–807, 1987.
22. Parker, J., Daniel, L. W., and Waite, M. Evidence of protein kinase C involvement in phorbol diester-stimulated arachidonic acid release and prostaglandin synthesis. J. Biol. Chem., *262:* 5385–5393, 1987.
23. Thompson, M. G., and Hickman, J. A. Elevation of HL-60 cell intracellular calcium by the cytotoxic ether lipid SRI 62-834 and antagonism by 12-*O*-tetradecylphorbol-13-acetate. Biochem. Soc. Trans., *16:* 278, 1988.
24. Lazenby, C. M., Thompson, M. G., and Hickman, J. A. Elevation of leukemic cell intracellular calcium by the ether lipid SRI 62-834. Cancer Res., *50:* 3327–3330, 1990.
25. Henson, P. M. Extracellular and intracellular activities of platelet activating factor. *In:* New Horizons in Platelet Activating Factor Research, pp. 3–10. Chichester: Wiley, 1987.
26. Kornecki, E., and Erlich, Y. H. Neuro regulatory and neuropathological actions of ether-phospholipid platelet-activating factor. Science (Washington, DC), *240:* 1792–1794, 1988.
27. Hallam, T. J., Sanchez, A., and Rink, T. J. Stimulus-response coupling in human platelets: changes evoked by platelet-activating factor in cytoplasmic free calcium monitored with the fluorescent indicator Quin 2. Biochem J., *218:* 819–827, 1984.
28. Hallam, T. J., and Rink, T. J. Agonists stimulate divalent cation channels in the plasma membrane of human platelets. FEBS Lett., *186:* 175–179, 1985.
29. Sawyer, D. B., and Anderson, O. S. Platelet-activating factor is a general membrane perturbant. Biochem. Biophys. Acta, *987:* 129–132, 1989.
30. Bazill, G. W., and Dexter, T. M. An antagonist to platelet activating factor counteracts the tumouricidal action of alkyl lysophospholipids. Biochem. Pharmacol., *38:* 374–377, 1989.
31. Lazenby, C. M., Dive, C., Thompson, M. G., and Hickman, J. A. The ether

[5] C. Dive, J. V. Watson, P. Workman, C. M. Lazenby, M. G. Thompson, and J. A. Hickman, unpublished observations.

lipid SRI 62-834 does not mimic the action of platelet activating factor. Proc. Am. Assoc. Cancer Res., *31:* 352, 1990.
32. Dive, C., Watson, J. V., and Workman, P. A multiparametric assay of membrane permeability by flow cytometry with complementary fluorescent probes. Cytometry, *11:* 244–252, 1990.
33. Casals-Stenzel, J., Maucevic, G., and Weber, K-H. Pharmacological actions of WEB 2086, a new specific antagonist of platelet activating factor. J. Pharmacol. Exp. Ther., *241:* 974–981, 1987.
34. Dive, C., Thompson, M. G., Hickman, J. A., Watson, J. V., and Workman, P. Specific biochemical or less-specific biophysical action of ether lipid SRI 62-834 on tumour cell membranes *in vitro*. Br. J. Cancer, *60:* 472, 1989.
35. Dive, C., Thompson, M., Hickman, J., Watson, J. V., and Workman, P. Simultaneous flow cytometric analysis of ether lipid SRI 62-834 modulation of membrane permeability and intracellular calcium homeostasis: evidence of a specific biochemical perturbation. Cancer Chemother. Pharmacol., *24* (Suppl. 2): 82, 1989.
36. Valone, F. H. Identification of platelet-activating factor receptors in P388D_1 murine macrophages. J. Immunol., *140:* 2389–2394, 1988.
37. Rockwell, S. C., Kallman, R. F., and Farjardo, L. E. Characteristics of a serially transplanted mouse mammary tumor and its tissue-culture-adapted derivative. J. Natl. Cancer Inst., *49:* 735–741, 1972.
38. Dive, C., Workman, P., and Watson, J. V. Improved methodology for intracellular enzyme reaction kinetics by flow cytometry. Cytometry, *8:* 552–561, 1987.
39. Musgrove, E., Rugg, C., and Hedley, D. Flow cytometric measurement of cytoplasmic pH: a critical evaluation of available fluorochromes. Cytometry, *7:* 347–355, 1986.
40. Watson, J. V. A method for improving light collection by 600% from square cross section flow cytometry chambers. Br. J. Cancer, *51:* 433–435, 1985.
41. Watson, J. V. Time, a quality control parameter in flow cytometry. Cytometry, *8:* 646–649, 1987.
42. Watson, J. V., Curling, O. M., Munn, C. F., and Hudson, C. N. Oncogene expression in ovarian cancer: a pilot study of c-*myc* oncoprotein in serous papillary ovarian cancer. Gynaecol. Oncol., *28:* 137–150, 1987.
43. Dive, C., Cox, H., Watson, J. V., and Workman, P. Polar fluorescein derivatives as improved substrate probes for flow cytoenzymological assay of cellular esterases. Mol. Cell. Probes, *2:* 131–145, 1988.
44. Mossman, T. Rapid colorimetric assay for cellular growth and survival: application to proliferation and cytotoxicity assays. J. Immunol. Methods, *65:* 55–63, 1983.
45. Twentyman, P. R., and Luscombe, M. A study of some of the variables in a tetrazolium dye (MTT) based assay for growth and chemosensitivity. Br. J. Cancer, *56:* 279–285, 1987.
46. Rink, T. J., Tsien, R. Y., and Pozzan, T. Cytoplasmic pH and free Mg^{2+} in lymphocytes. J. Cell Biol., *95:* 189–196, 1982.
47. Seewald, M. J., Olsen, R. A., Sehgal, I., Melder, D. C., Modest, E. J., and Powis, G. Inhibition of growth factor-dependent inositol phosphate Ca^{2+} signaling by antitumor ether lipid analogues. Cancer Res., *50:* 4458–4463, 1990.